Design of polarization-maintaining retro-reflector for folded-path applications

Zhen Guo (郭 振)[1] , Lianshan Yan (闫连山)[1*], Wei Pan (潘 炜)[1], Bin Luo (罗 斌)[1], Kunhua Wen (温坤华)[1], and X. Steve Yao[2]

[1] *Center for Information Photonics and Communications, School of Information Science and Technology, Southwest Jiaotong University, Chengdu 610031, China*

[2] *General Photonics Corp., 5228, Edison Ave., Chino, CA 91710, USA*

[*] *Corresponding author: lsyan@home.swjtu.edu.cn*

Received March 3, 2011; accepted April 21, 2011; posted online July 11, 2011

A design of polarization-maintaining retro-reflectors (PMRRs) for folded-path applications is proposed and analyzed. The prism-based scheme enables the output light, which is parallel to the input, to have an identical state of polarization. The principle of the design is theoretically verified, and the related error is analyzed due to possible manufacturing imperfection. The maximum spatial angle error is $\pm 2.75^\circ$. The effect on the extinction ratio and insertion loss is also discussed, which further proves the design's feasibility in practical applications.

OCIS codes: 060.2420, 230.5440, 260.5430.
doi: 10.3788/COL201109.100601.

Polarization maintaining reflectors play an essential role in physical optics and optical communications. However, the phase shift induced by the reflection may affect the state of polarization (SOP) of signals. The SOP is essential information in optical sensors and ellipsometers[1−5]. Thus, maintaining the reflecting polarization is crucial and has attracted much attention. However, most of these applications are based on the coating technology[6−9] and the design of photonic crystal[10−13], which are not appropriate in practical applications because of the special equipment or high precision required. Clearly, the most efficient approach to overcome the effect is to employ no-shift instruments[14−16], which are easy to fabricate and implement in practical applications.

In this letter, we propose a novel design of polarization-maintaining retro-reflector (PMRR) for folded-path applications. Four spatial reflectors are employed to interchange the reflection coefficients of both polarizations to achieve polarization maintaining. The parallelization between the input and output lights can be realized geometrically. The theoretical background is presented. The transmission coefficient after four reflections are proven to be the same based on the Jones matrix. The fabrication error in practical application is then considered. The calculation results show that the maximum spatial angle error is $\pm 2.75^\circ$. The error effect on the extinction ratio and insertion loss of the input polarized light is also discussed. The feasibility can be easily achieved in the current technology based on the results.

The ordinary total internal reflection can induce unexpected phase shifts, which change the SOP of the output. When a polarized monochromatic beam propagates to the total reflection interface, the transmission characteristics can be modeled in the Jones space as follows:

$$\begin{bmatrix} E_{\mathrm{r}}^{\mathrm{p}} \\ E_{\mathrm{r}}^{\mathrm{s}} \end{bmatrix} = \begin{bmatrix} r_{\mathrm{p}} & 0 \\ 0 & r_{\mathrm{s}} \end{bmatrix} \begin{bmatrix} E_{\mathrm{i}}^{\mathrm{p}} \\ E_{\mathrm{i}}^{\mathrm{s}} \end{bmatrix}, \tag{1}$$

where r_{p} and r_{s} represent the reflection coefficients of the horizontal and perpendicular components, respectively. The two coefficients are usually not exactly the same. Thus, utilizing the simple right-angle prism to realize the reflection could induce change in the SOP of the output. The different phase shifts δ can be derived from the Fresnel equation:

$$\tan\frac{\delta}{2} = \frac{\cos\theta_{\mathrm{i}}\sqrt{\sin^2\theta_{\mathrm{i}} - n^2}}{\sin^2\theta_{\mathrm{i}}}, \tag{2}$$

where $n = n_2/n_1$ denotes the light propagating from media 1 to 2, and θ_{i} is the incident angle. The amplitude of the total reflected wave is equal to the incident wave, but its phase is shifted by an amount determined byδ.

The polarization maintaining cannot be satisfied by a simple reflection according to Eqs. (1) and (2). To achieve the same SOP between the input and output lights, orthogonal components should have an identical reflection coefficient. If the two reflection surfaces are orthogonal to each other, as shown in Fig. 1(a), the transmission coefficients r_{p} and r_{s} can be interchanged by plumbing the two reflection surfaces. Therefore, the entire coefficients after two reflections of the two components are both $r_{\mathrm{p}} \cdot r_{\mathrm{s}}$.

The aim of this work is to design a PMRR. The input and output lights are not only required to perform the same SOP but also to be parallel. Based on the two-orthogonal model, we propose a four-reflection model, as shown in Fig. 1(b). Not only the same phase shift for the horizontal and perpendicular components but also the parallelization between the input and output lights can be realized. First, all the incident angles of the four reflectors must be the same; thus, r_{s} and r_{p} are identical for the four times reflections. The first reflector is set to $\pi/4$ on the horizontal surface, and the input light is set along the vertical axis. The light is then reflected to the second parallel reflector. To exchange r_{s} and r_{p}, the second one is set orthogonally on the horizontal surface

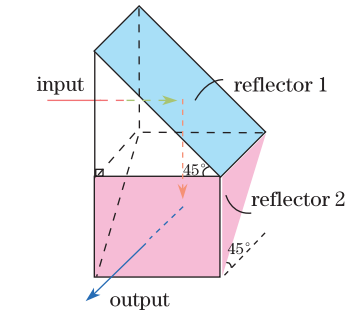

(a)

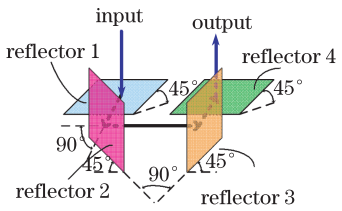

(b)

Fig. 1. (a) Polarization-maintaining reflector of two reflectors; (b) principle of the PMRR. The three-dimensional (3D) illustration shows light propagation with total-internal-reflection (TIR) on four-reflection surfaces.

and $\pi/4$ along the y axis. Therefore, the transmission matrix should become

$$\begin{bmatrix} r_{\rm s} & 0 \\ 0 & r_{\rm p} \end{bmatrix}. \tag{3}$$

Then, the output can be derived as

$$\begin{bmatrix} E_{\rm r}^{\rm p} \\ E_{\rm r}^{\rm s} \end{bmatrix} = \begin{bmatrix} r_{\rm p} & 0 \\ 0 & r_{\rm s} \end{bmatrix} \begin{bmatrix} r_{\rm s} & 0 \\ 0 & r_{\rm p} \end{bmatrix} \begin{bmatrix} r_{\rm s} & 0 \\ 0 & r_{\rm p} \end{bmatrix} \begin{bmatrix} r_{\rm p} & 0 \\ 0 & r_{\rm s} \end{bmatrix} \begin{bmatrix} E_{\rm i}^{\rm p} \\ E_{\rm i}^{\rm s} \end{bmatrix}$$

$$= \begin{bmatrix} r_{\rm p}r_{\rm s}r_{\rm s}r_{\rm p} & 0 \\ 0 & r_{\rm s}r_{\rm p}r_{\rm p}r_{\rm s} \end{bmatrix} \begin{bmatrix} E_i^p \\ E_i^s \end{bmatrix}. \tag{4}$$

The four reflectors are shown in Fig. 1(b). The changes in the two components are $r_{\rm p}r_{\rm s}r_{\rm s}r_{\rm p}$. Thus, theoretically, we prove that the two orthogonal polarizations share the same change in the phase. Clearly, the parallelization of the input and output lights can be easily proven geometrically. We can obtain the retro-reflection with polarization maintaining for folded-path application using the design.

Although the purpose of the study is to design a PMRR, technological feasibility is another important aspect that should be considered. Based on the schematic diagram in Fig. 1(b), a fixed prism including four reflectors can be employed to implement the model, as shown in Fig. 2. The material of the prism can be fused silica. An anti-reflection (AR) coating with dual windows of 1 300 and 1 550 nm (R<0.5%) can be added at the interface. One of the difficulties in using the prism is obtaining the angular accuracy. Based on the combination of the four reflectors, a tiny spatial error may lead to an inevitable fluctuation of the output.

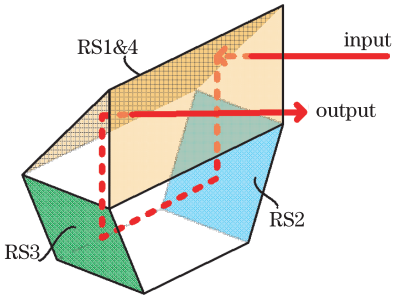

Fig. 2. cheme of the single-fixed prism surfaces. RS:reflecting surface

In practical applications, the fabrication error of the angle can be limited within 30′ Although the input interface before reflection 1 in Fig. 2 does not introduce any distortion in the phase, the influence on the following reflectors cannot be neglected. The angle error of the input interface shown in Fig. 2 is

$$f_0(\theta_1) = \theta_1. \tag{5}$$

The next four reflections can be derived. The error in the angle induced by RS1 (RS:reflcting surface) and f_0 is

$$f_1(\theta_1, \theta_2) = \frac{\pi}{4} + f_0 - \arcsin\left(\frac{\sin(f_0)}{n_1}\right) + \theta_2. \tag{6}$$

The error after RS2 and RS3 can be derived as

$$f_2(\theta_1, \theta_2, \theta_3) = \arccos\left(\frac{\cos(f_1 - \frac{\pi}{4})}{\sqrt{2}}\right) + \theta_3, \tag{7}$$

$$f_3(\theta_1, \theta_2, \theta_3, \theta_4) =$$
$$\arccos\left(\frac{-\cos(2 \times f_2 + \arccos(\sqrt{\frac{1+\sin^2(f_1-\frac{\pi}{4})}{2}}))}{\sqrt{2 \times \tan^2(f_1 - \frac{\pi}{4}) + 1}}\right) + \theta_4. \tag{8}$$

After the light reflects from RS4 back to the input and output surfaces, the transmission through the surface does not induce any phase change of the two polarizations. Thus, the inaccuracy induced by the interface can be neglected. All fabrication errors can be derived as

$$f_4(\theta_1, \theta_2, \theta_3, \theta_4, \theta_5) = \frac{a1 + a2 + a3 + a4}{b}, \tag{9}$$

where $a1, a2, a3, a4$, and b are

$$a1 = 4 \times \tan^2(f_3) - 8 \times \tan^2(f_1 - \frac{\pi}{4}) + \frac{1}{4 \times \cos^2(f_3)},$$

$$a2 = -(\sqrt{(2 \times \tan^2(f_3) - 4 \times \tan^2(f_1 - \frac{\pi}{4}))} + \frac{\sqrt{2}}{2 \times \tan(f_1 - \frac{\pi}{4})})^2,$$

$$a3 = -(2 \times \tan^2(f_1 - \tfrac{\pi}{4}) + 1) \times \tan^2(\arccos(-\cos(2 \times f_2 + \arccos(\sqrt{\frac{1 + \sin^2(f_1 - \frac{\pi}{4})}{2}})))))/4,$$

$$a4 = -(\tfrac{1}{2} - 2 \times \sqrt{\tfrac{1}{4} \times \tan^2(f_3) - \tfrac{1}{2} \times \tan^2(f_1 - \tfrac{\pi}{4})})^2,$$

$$b = 2\sqrt{4 \times \tan^2(f_3) - 8 \times \tan^2(f_1 - \frac{\pi}{4})} \times \sqrt{\frac{1}{4 \times \cos^2(f_3)}}. \tag{10}$$

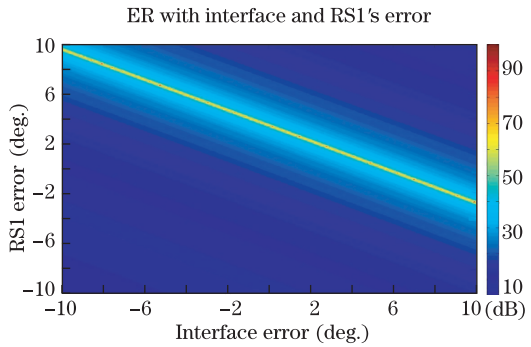

Fig. 3. ER with the fabrication error of the input-surface and RS1.

The deviation spatial angle of the output can be determined by the equations shown above. The maximum error is $\pm 2.75°$, which is allowable in practical application. We now discuss the effect of the fabrication error on the extinction ratio (ER) of the polarized light. The initial ER of the input is 20 dB. All situations of the fabrication error of the four reflectors can be obtained. The calculation results show that the worst ER is 16.24 dB, which is also acceptable in the industry. However, the curves are too complex to express the ER with five variables. Only the error of the interface and reflector 1 is considered; the simulation result is shown in Fig. 3. Note that the error is arranged $[-10°, 10°]$ to reflect the overall trend. The ER curve of the error area $[-0.5°, 0.5°]$ is flat and has no upheaval, proving the stability of the design. Accuracy can be further improved by reducing the manufacturing error of the spatial angle.

Insertion loss is another key parameter of optical devices. There are two kinds of losses in the proposed structure: loss of input surface and reflection loss of RS1–RS4 in Fig. 2. An AR coating (R<0.5%) is added on the interface, and thus the interface loss is set to 0.5%. The reflection loss of RS1–RS4 in practical application is set to 2%, and thus the insertion loss of the structures is -0.91 dB based on the current industry. Based on the discussion above, the feasibility can be easily achieved through the imperfection of the current manufacturing.

The design presented here can be effectively used in practical applications because of its novel folded-path design. Another great advantage is its concision, which is made up of fixed prisms. The following are some application examples.

(i) The prism shown above needs only four reflectors. The manufacturing process is easy to implement. Thus, not only can the size be changed but also the shape of our design to adapt to different needs, as shown in Fig. 4(a).

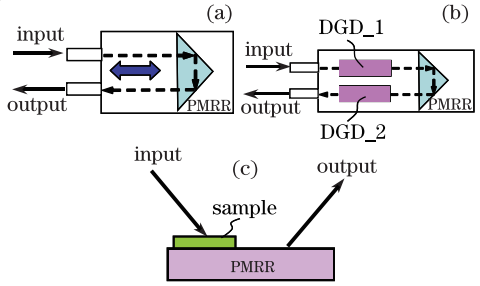

Fig. 4. Practical applications based on the PMRR design. (a) PMRR; (b)1st PMD-emulator without inducing the high-order effect; (c) ellipsometer.

(ii) The polarization mode dispersion (PMD) emulator (Fig. 4 (b)) is very important in the testing of new technology with PMD in the system. Rapidly exploring the number of fiber ensembles to determine the PMD-induced outages is impossible. With the PMRR in the differential-group-delay (DGD) (first order of the PMD) emulator, the length can be divided into two parts to reduce the size without inducing any high-order effect.

(iii) Ellipsometers are another important application based on polarization[17] (Fig. 4 (c)). Based on the scheme discussed above, if there are no phase shifts induced by the reflection, and the input polarization is fixed, we can test the characteristics of the samples, which can be the surface of a metal or bio-film, after analyzing the polarization of the output light.

$$\tan\varphi \cdot \mathrm{e}^{\mathrm{i}\Delta} = \left|\left(\frac{A_\mathrm{p}}{A_\mathrm{s}}\right)_\mathrm{r}\right| \cdot \mathrm{e}^{\mathrm{i}(\theta_\mathrm{p}-\theta_\mathrm{s})}, \tag{11}$$

where Δ is the phase shift, and $A_\mathrm{p}/A_\mathrm{s}$ is the amplitude ratio. Through the PMRR, the shifts induced by the reflection can only be eliminated, and the differences between input and the output can be induced by the samples.

In conclusion, a novel PMRR design for folded-path application, which is easier to implement in practical applications, is proposed. The principle of the design is clear, and the simulations results agree well with the design. Based on the error analysis, the feasibility can be easily achieved with the current technology. Accuracy can be further improved by increasing the precision.

This work was supported by the Program for New Century Excellent Talents in the University of Ministry of Education of China (No. NCET-08-0821), the Research Project in Sichuan Province of China (No. 2010HH0009), and the State Key Lab of Optical Technologies for Micro-Engineering and Nano-Fabrication of China. The original idea was initiated in General Photonics Corp.[18,19], with contributions from Dr. Steve Yao, Dr. James Chen, and Ms. Lynn Lin.

References

1. D. Goldstein, *Polarized Light* (2nd edition) (Marcel Dekker, New York, 2003).
2. E. Collett, *Polarized Light*: *Fundamentals and Applications* (Marcel Dekker, New York, 1993).
3. M. Born and E. Wolf, *Principle of Optics*: *Electromagneti c Theory of Propagation, Interference and Diffraction of Light* (7th edition) (University Press, Cambridge, 1999).
4. H. Hao, B. Li, W. Wang, and B. Yin, Chin. Opt. Lett. **8,** 108 (2010).
5. J. Ye, L. Yan, A. Yi, W. Pan, B. Luo, Z. Guo, and X. S. Yao, Chin. Opt. Lett. **8,** 979 (2010).
6. K. B. Rochford, A. H. Rose, M. N. Deeter, and G. W. Day, Opt. Lett. **19,** 1903 (1994).
7. A. Thelen, Appl. Opt. **15,** 2983 (1976).
8. T. Yoshino, M. Gojyuki, Y. Takahashi, and T. Shimoyama, Appl Opt. **36,** 5566 (1997).
9. Z. P. Wang, Z. J. Huang, C. Kang, W. M. Sun, S. L. Ruan, Y. H. Luo, A. W. Palmer, and K. T. V. Grattan,

Opt. Laser Technol. **31,** 455 (1999).
10. D. R. Solli, C. F. McCormick, R. Y. Chiao, and J. M. Hickmann, J. Appl. Phys. **93,** 9429 (2003).
11. D. R. Solli, C. F. McCormick, R. Y. Chiao, and J. M. Hickmann, Opt. Express **11,** 125 (2003).
12. H. Fang, S. Luo, T. Guo, and S. Jian, Chin. Opt. Lett. **4,** 508 (2006).
13. Y. Zhang, Y. Shen, J. Zhou, Y. Wang, F. Wu, J. Sun, and C. Guo, Chin. Opt. Lett. **9,** 022001 (2011).
14. M. Gilo, Appl. Opt. **31,** 5345 (1992).
15. T. Sato, G. Takahashi, and I. Yoshiaki, Method and apparatus for optically measuring a current", U.S. Patent 4564754 (1986).
16. C. Li, C. Zhang, N. Song, and H. Xu, Chin. Opt. Lett. **9,** 020604 (2011).
17. T. A. Germer, Phys. Rev. Lett. **85,** 349 (2000).
18. L. Yan, X. Chen, and X. S. Yao, Optical differential group delay module with folded optical path" U.S. Patent 7723670 B1 (2010).
19. X. S. Yao, X. Chen, T. Xia, G. Wellbrock, D. Chen, D. Peterson, P. Zhang, A. Belisle, L. Dong, and T. Yu, Opt. Express **18,** 27306 (2010).